# Cosmology from EoR/Cosmic Dawn

**Pritchard**[*][†]**, Chang, Furlanetto, Choudhury, Zaroubi, Santos, Chen, Weller, Abdalla, Mesinger, Metcalf on behalf of the Cosmology-SWG and EoR/CD-SWG**
*Imperial College London*
*E-mail:* j.pritchard@imperial.ac.uk

**Robert Benton Metcalf**
*Dipartimento di Fisica e Astronomia, Universitá di Bologna, viale B. Pichat 6/2 , 40127, Bologna, Italy*
*E-mail:* robertbenton.metcalf@unibo.it

**Alkistis Pourtsidou**
*Dipartimento di Fisica e Astronomia, Universitá di Bologna, viale B. Pichat 6/2 , 40127, Bologna, Italy*
*E-mail:* alkistis.pourtsidou@unibo.it

SKA Phase 1 will build upon early detections of the EoR by precursor instruments, such as MWA, PAPER, LOFAR, and HERA, to make the first high signal-to-noise measurements of fluctuations in the 21 cm brightness temperature from both reionization and the cosmic dawn. This will allow both imaging and statistical maps of the 21cm signal at redshifts $z = 6 - 30$ and constrain the underlying cosmology and evolution of the density field. This era includes nearly 60% of the (in principle) observable volume of the Universe and many more linear modes than the CMB, presenting an opportunity for SKA to usher in a new level of precision cosmology. This optimistic picture is complicated by the need to understand and remove the effect of astrophysics, so that systematics rather than statistics will limit constraints.

This chapter will describe the cosmological, as opposed to astrophysical, information available to SKA Phase 1. Key areas for discussion include: cosmological parameters constraints using 21cm fluctuations as a tracer of the density field; lensing of the 21cm signal, constraints on heating via exotic physics such as decaying or annihilating dark matter; impact of fundamental physics such as non-Gaussianity or warm dark matter on the source population; and constraints on the bulk flows arising from the decoupling of baryons and photons at $z = 1000$. The chapter will explore the path to separating cosmology from 'gastrophysics', for example via velocity space distortions and separation in redshift. We will discuss new opportunities for extracting cosmology made possible by the sensitivity of SKA-1 and explore the advances achievable with SKA-2.

---

[*]Speaker.

[†]A footnote may follow.

# 1. Introduction

The years since the COBE observations of the CMB have ushered in an age of precision cosmology. Key cosmological parameters have been made possible by measurements of the distribution of matter in the Universe through WMAP and Planck observations of CMB anisotropies and large volume galaxy surveys such as SDSS. These surveys have made precision measurements of parameters describing the matter content of the Universe - the baryons $\Omega_b$, dark matter $\Omega_c$, dark energy $\Omega_\Lambda$, radiation $\Omega_r$, and neutrinos $\Omega_v$ - and the physics of inflation - via the tilt $n_s$, amplitude $A_s$, running $dn_s/d\log k$ or the primordial potential power spectrum and $r$ the ratio of tensor-to-scalar modes produced by inflation. These measurements have firmly established the basic picture of our Universe, known widely as the $\Lambda$CDM model of cosmology.

Despite this progress, measuring these numbers is only the first step towards a deep understanding of the underlying physics. Our ignorance of the nature of the dark matter and the dark energy or how neutrinos acquire mass and what value that mass takes are just two questions that modern cosmology hopes to address. Over the next decade two paths will help shed light on this. The simplest is simply to measure these cosmological parameters ever more precisely and over a wider range of times and scales in the hope of gaining further insights. The exemplar of this is with dark energy, where attempts to measure the redshift evolution of the dark energy density, parameterised by an equation of state $w(z)$, might distinguish a true cosmological constant from more general dark energy or modified gravity. For others there are critical thresholds of precision required to distinguish physical scenarios - for example, measuring the sum of the neutrino masses $M_v \lesssim 0.1$ would determine the neutrino mass hierarchy. Clearly more precision is a good thing, but it is not the only path forward.

Secondly, we can seek signatures of new physics in ways distinct from the distribution of large scale matter. The processes that produce dark matter will also allow it to annihilate and maybe to decay. The release of energy might have impact on the surrounding environment, heating the intergalactic medium. Pursuing unique signatures of new physics in new regimes will be a key part of the next decade.

The SKA is uniquely placed to probe cosmology as it is capable of mapping the Universe over wide volumes and an unprecedented range of redshifts. Figure 1 illustrates the additional range of volume and redshifts that the SKA will constrain. In this chapter, we will focus on the new opportunities created by SKA observations of the epoch of reionization (EoR) and the cosmic dawn (CD). This period has never before been observed offering a unique opportunity to test the consistency of the $\Lambda$CDM model and search for new hints to the great unanswered questions of cosmology.

[1]

# 2. Cosmological parameters from density fluctuations

### Introduce fisher matrix formalism

In this section, we explore the ability of SKA to constrain cosmological parameters via observations of the density field. Just as galaxy surveys constrain cosmology by using galaxies as a tracer of the linear density field, SKA can constrain cosmology by using the 21 cm brightness
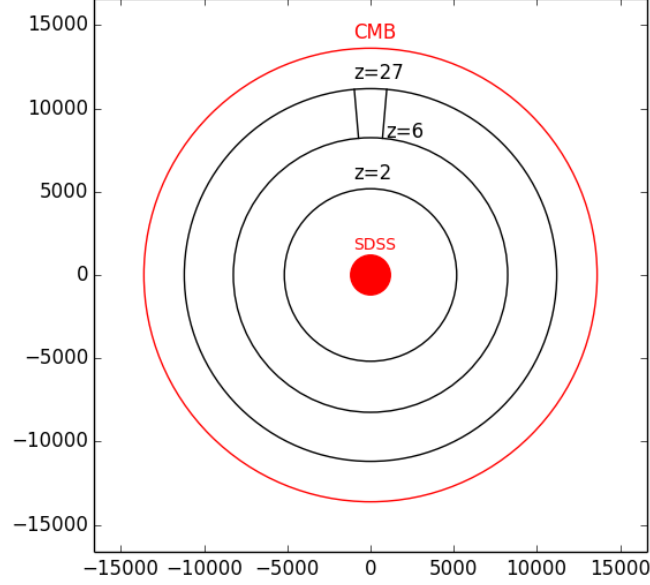
**Figure 1:** Illustration of the volume probed by SKA

temperature as a tracer of the density field. This is not an unproblematic assertion, since brightness temperature fluctuations may be sourced by variation in the spin temperature and neutral fraction in addition to the density field.

$$\delta T_B = (1+\delta)x_H...$$ (2.1)

Equation 2.1 shows how these different terms come into play. In a regime where $T_S \gg T_{\text{CMB}}$ and $x_H = 1$ then $\delta T_B$ will be an unbiased tracer of the density field. At all other times the effects of astrophysics must be modelled and removed or somehow avoided. We will return to a discussion of this point in §7 as this is a critical point.

In this section, we take the optimistic view that there will a regime in which $\delta T_b \propto (1+\delta)$ so that the 21cm signal provides a clean measurement of the density field. This approach enables us to evaluate the best case scenario for SKA in measuring cosmological parameters. By comparing this to galaxy surveys we get a sense of how competitive SKA could be, if astrophysics could be overcome.

The sensitivity of a radio interferometer to the 21cm power spectrum has been well studied [?, ?, ?] and we follow the same approach here. The variance of a 21 cm power spectrum estimate for a single **k**-mode with line of sight component $k_{||} = \mu k$ is given by [?]:

$$\sigma_P^2(k,\mu) = \frac{1}{N_{\text{field}}} \left[ \bar{T}_b^2 P_{21}(k,\mu) + T_{\text{sys}}^2 \frac{1}{Bt_{\text{int}}} \frac{D^2 \Delta D}{n(k_\perp)} \left( \frac{\lambda^2}{A_e} \right)^2 \right]^2.$$ (2.2)

The first term on the right-hand-side of the above expression provides the contribution from sample variance, while the second describes the thermal noise of the radio telescope. The thermal noise depends upon the system temperature $T_{\text{sys}}$, the survey bandwidth $B$, the total observing time $t_{\text{int}}$, the conformal distance $D(z)$ to the center of the survey at redshift $z$, the depth of the survey $\Delta D$, the observed wavelength $\lambda$, and the effective collecting area of each antennae tile $A_e$. The effect of the configuration of the antennae is encoded in the number density of baselines $n_\perp(k)$ that observe a mode with transverse wavenumber $k_\perp$ [**?**]. Observing a number of fields $N_{\text{field}}$ further reduces the variance.

Estimates of the error on a power spectrum measurement are calculated using the Fisher matrix formalism, so that the $1 - \sigma$ errors on the model parameter $\lambda_i$ are $(\mathbf{F}_{ij}^{-1})^{1/2}$, where

$$F_{ij} = \sum_\mu \frac{\varepsilon k^3 V_{\text{survey}}}{4\pi^2} \frac{1}{\sigma_P^2(k,\mu)} \frac{\partial P_{T_b}}{\partial \lambda_i} \frac{\partial P_{T_b}}{\partial \lambda_j}. \tag{2.3}$$

In this equation, $V_{\text{survey}} = D^2 \Delta D (\lambda^2/A_e)$ denotes the effective survey volume of our radio telescopes and we assume wavenumber bins of width $\Delta k = \varepsilon k$. We will be interested in the cases where $\lambda_i = \{\bar{P}_{T_b}\}$ and $\lambda_i = \{P_{\mu^0}, P_{\mu^2}, P_{\mu^4}\}$.

**sensitivity plot for various experiments relative to density field**

**Table 1:** Low-frequency radio telescopes and their parameters. We specify the number of antennae $N_a$, total collecting area $A_{\text{tot}}$, bandwidth $B$, and total integration time $t_{\text{int}}$ for each instrument. These values are fixed at $z =$?? and extrapolated to other frequencies using $A_{\text{tot}} = N_{\text{ant}} N_{\text{dip}} A_{\text{dip}}$ with the number of antennae per station $N_{\text{dip}} = 289$ and $A_{\text{dip}} = \min(\lambda^2/3, 3.2\,\text{m}^2)$.

| Array | $N_a$ | $A_{\text{tot}}(10^3\,\text{m}^2)$ | $B$ (MHz) | $t_{\text{int}}$ (hr) | $R_{\min}(m)$ | $R_{\max}(km)$ |
|---|---|---|---|---|---|---|
| MWA | 112 | 1.6 | 8 | 1000 | 4 | 0.75 |
| LOFAR Core | 48 | 38.6 | 8 | 1000 | 100 | 1.5 |
| HERA | 331 | 50.0 | 8 | 1000 | 14.3 | 0.3 |
| SKA0 | 850×0.5 | 224×0.5 | 8 | 1000 | 35 | 2 |
| SKA1 | 850 | 224 | 8 | 1000 | 35 | 1 |
| SKA2 | 850×4 | 224×4 | 8 | 1000 | 35 | 2 |

We first illustrate the sensitivity of different iterations of SKA in Figure 2, where we take the parameters in Table 1 for SKA0 - with 50% of the SKA1 baseline collecting area, SKA1, and SKA2 - with x4 the collecting area of SKA1. For each of these we assume a filled core of radius $R_{\max}$ and ignore all antennae outside this distance.

**SKA1 has 911 stations total with 899 in the core and 650 stations within a radius of 1km accounting for 75% of the total number of stations and collecting area. Physical station size is 35m. Stations have 289 antennae with antennae area $A_e = \lambda^2/3$ giving $3.2m^2$ at 110MHz. At lower frequencies the array is densely packed and has constant collecting area, at higher frequencies the array becomes sparse.**

Figure 2 illustrates a few key points governing parameter constraints. The large station sizes remove sensitivity to the largest physical scales (smallest $k$ modes). By $z = 20$ the amplitude of the
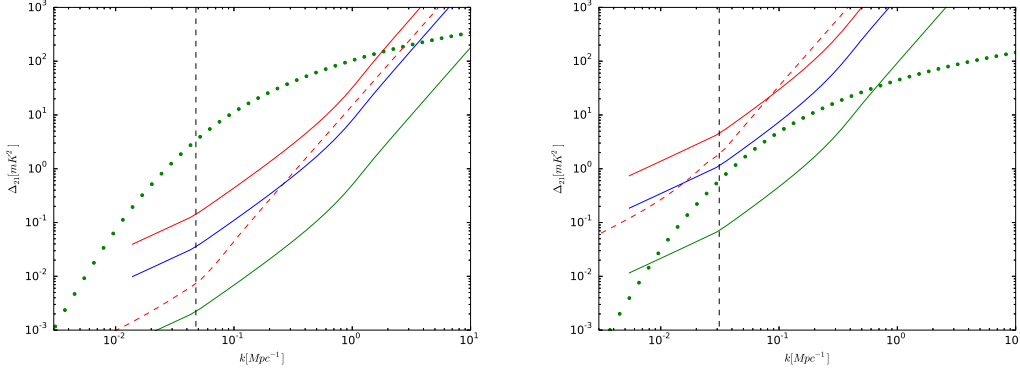
**Figure 2:** Sensitivity plots of HERA (red dashed curve), SKA0 (red), SKA1 (blue), and SKA2 (green). Dotted curve shows the predicted 21cm signal from the density field alone assuming $x_H = 1$ and $T_S \gg T_{CMB}$. Vertical black dashed line indicates the smallest wavenumber probed in the frequency direction $k = 2\pi/y$, which may limit foreground removal. *Left panel: $z = 8$ Right panel: $z = 20$.*

21 cm signal is too small to be detected by SKA1 *if we assume $T_S \gg T_\gamma$.* Detection of the 21cm signal at $z \gtrsim 20$ with SKA1 is dependent upon a strong 21cm absorption signal that boosts the amplitude of the 21cm power spectrum. Unfortunately, it seems likely that during the absorption regime the details and spatial variation of the spin temperature will matter and complicated getting at cosmology.

    **concept of effective volume and how SKA compares to various galaxy surveys**

    The key parameters for determining cosmological parameters are the effective volume probed and the minimum wavenumber probed $k_{min}$ where modes can still be assumed to be linear. SKA has a significant advantage over galaxy surveys as more modes are still in the linear regime at $z > 6$. We set $k_{min} = 2 \mathrm{Mpc}^{-1}$ **justify or do better**

**Figure 3:** Effective volume and comparison of SKA to Euclid

    Comment on higher redshift giving other advantages, eg isocurvature, where effects become smaller deeper into matter dominated regime.

    Table 2 shows the cosmological parameters obtained with the listed experimental performances.

## 2.1 Core cosmological parameters

## 2.2 Inflationary parameters

## 2.3 Neutrino mass

## 3. Constraining new physics from heating

    Dark stars?

**Table 2:** Fiducial parameter values and $1 - \sigma$ experimental uncertainties for cosmological parameters. Dashes indicate parameters not relevant for that experiment; $\infty$ indicates parameters that are relevant, but not constrained.

| | $\Omega_m h^2$ | $\Omega_b h^2$ | $\Omega_\Lambda$ | $w$ | $n_s$ | $A_s^2$ | $\tau$ | $Y_{He}$ | $M_\nu$ |
|---|---|---|---|---|---|---|---|---|---|
| Fiducial | 0.147 | 0.023 | 0.7 | -1 | 0.95 | 26.6 | 0.1 | 0.24 | 0.3 |
| SDSS | 0.456 | 0.083 | 0.117 | 1.21 | 0.503 | $\infty$ | … | … | |

## 4. Fundamental physics from modifications to the source population

## 5. Bulk flows

## 6. Cosmic shear and the EoR

It is possible that the EoR signal could be used to measure weak gravitational lensing. In [2] and [3] it was shown that if the EoR is at redshift $z \sim 8$ or later, a large radio telescope such as the SKA could measure the lensing convergence power spectrum. However a very large $f_{sky}$ and a very compact low frequency array was assumed by those authors. Here the calculation is repeated with parameters that are more consistent with current SKA plans. The current plans for a 25 square degree survey with SKA_Low will preclude measuring cosmological parameters through their effects on the weak lensing power-spectrum because of large sample variance. (This is not true of the SKA_Mid at lower redshift where the survey area will be much larger. See section \*\*\* for more details.) It still might be possible to map the lensing convergence within the 25 square degree EoR survey area. This would allow us to actually "see" the distribution of dark matter in a typical region of the sky, something that is only possible with galaxy lensing around very atypical, large galaxy clusters.

The previously mentioned authors extended the Fourier-space quadratic estimator technique, which was first developed in [4] for CMB lensing observations to three dimensional observables, i.e. the 21 cm intensity field $I(\theta, z)$. The convergence estimator and the corresponding lensing reconstruction noise are calculated assuming that the temperature (brightness) distribution is Gaussian. This will not be strictly true during the EoR, but serves as a reasonable approximation for these purposes. Note that the lensing reconstructions noise contains the thermal noise of the telescope which is calculated using the formula

$$C_\ell^N = \frac{(2\pi)^3 T_{sys}^2}{\Delta \nu t_{obs} f_{cover}^2 \ell_{max}(\nu)^2} \, , \qquad (6.1)$$

where the system temperature $T_{sys}$ at high redshifts is dominated by galactic synchrotron radiation, $\Delta \nu$ is the chosen frequency window, $t_{obs}$ the total observation time, $D_{tel}$ the diameter (maximum baseline) of the core array and $\ell_{max}(\lambda) = 2\pi D_{tel}/\lambda$ is the highest multipole that can be measured by the array at frequency $\nu$ (wavelength $\lambda$). $f_{cover}$ is the total collecting area of the core array $A_{coll}$ divided by $\pi(D_{tel}/2)^2$. For SKA_Low we can consider a $1,000$ hr observation time and we choose $\Delta \nu = 10 \, \text{MHz}$, but with multiple bands that can be stacked to reduce the noise.

We assuming the SKA1 Baseline Design [5] parameters of $A_{\mathrm{coll}} \simeq 0.4\,\mathrm{km}^2$ with maximum baseline $D_{\mathrm{tel}} = 6\,\mathrm{km}$ and a more compact configuration of $A_{\mathrm{coll}} = 0.75\,\mathrm{km}^2$, $D_{\mathrm{tel}} = 2\,\mathrm{km}$. The estimated lensing noise is shown in Figure 4 along with the estimated signal. Here $C_L$ is the displacement field power spectrum and $N_L$ the lensing reconstruction noise assuming a reionization fraction $f_{\mathrm{HI}} = 1$ at the source redshift $z_s = 8$.
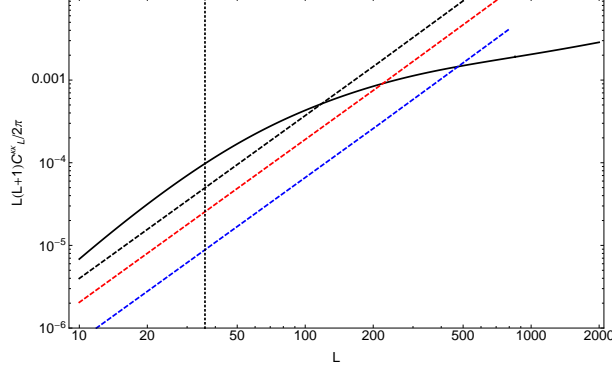


**Figure 4:** The lensing displacement field power spectrum, $C_L$, for sources at $z = 8$ is shown as a solid black line and lensing reconstruction noise $N_L$ as dashed lines. The black dashed curve is for the Baseline Design with 20 5 MHz frequency bins around $z = 8$ spanning the redshift range $z = 6 - 12$. The blue line is for the more compact array ($D_{\mathrm{tel}} = 2\,\mathrm{km}$) and the same frequency bins. The red line is the same as the blue but with 10 5 MHz frequency bins instead of 20, spanning the redshift range $z = 7 - 10$. The vertical line is approximately the lowest $L$ accessible with a 5-by-5 degree field. Where the noise curves are below $C_L$ typical fluctuations in the lensing deflection should be recoverable in a map.

These results show that it might be possible to map the lensing signal over a range of angular scales. This measurement would greatly benefit from a more compact array and/or the large collecting area that will come with Phase 2. The weak lensing power spectrum can be better measured for redshifts after reionization using SKAMid and the same 21 cm intensity mapping technique discussed, but over a much larger area of sky [6].

## 7. Separating "gastrophysics" and cosmology

The key challenge for extracting fundamental physics from the 21cm signal will be separating the effects of cosmology from "gastrophysics". A number of avenues have been studied in the literature, which broadly separate into (1) avoidance and (2) modelling. In the absence of a clearly defined window where $T_S \gg T_{\mathrm{CMB}}$ and $x_H = 1$ it might still be possible to avoid astrophysics via the angular dependence of the power spectrum induced by redshift space distortions. Focussing on the $P_{\mu^4} \approx P_\delta$ part could lead to clean cosmological measurements. Obtaining precision cosmology this way is hard and the literature suggests little improvement over Planck is possible [7, 8]. Figure 5 shows predicted errors bars for SKA1 on the $P_{\mu^2}$ and $P_{\mu^4}$ parts of the power spectrum. A detection is possible with reasonable sensitivity.

Information in $P_{\mu^2}$ is likely to help with modelling of the astrophysics.

Compared with the CMB our theoretical understanding of the 21cm signal during reionization is poor. Predictions for the 21cm power spectrum do not exist at the same level of precision as the
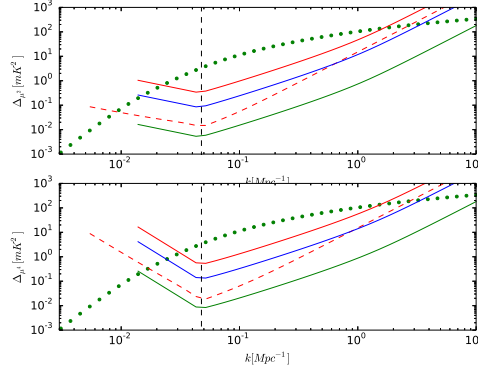
**Figure 5:** Sensitivity plots on $P_{\mu^2}$ and $P_{\mu^4}$ for HERA (red dashed curve), SKA0 (red), SKA1 (blue), and SKA2 (green). Dotted curve shows the predicted 21cm signal from the density field alone assuming $x_H = 1$ and $T_S \gg T_{\text{CMB}}$. Vertical black dashed line indicates the smallest wavenumber probed in the frequency direction $k = 2\pi/y$, which may limit foreground removal. *Left panel: $z = 8$ Right panel: $z = 20$.*

cosmology. Nonetheless, we expect the contribution of astrophysics to be relatively broad band and determined by extra power about a characteristic scale, eg the bubble size during reionization.

## 8. Paths to cosmology with Phase 1 and Phase 2

## 9. Miscellaneous?

## References

[1] S. R. Furlanetto, S. P. Oh, and E. Pierpaoli. Effects of dark matter decay and annihilation on the high-redshift 21cm background. *PRD*, 74(10):103502, November 2006.

[2] O. Zahn and M. Zaldarriaga. Lensing Reconstruction Using Redshifted 21 Centimeter Fluctuations. *ApJ*, 653:922–935, December 2006.

[3] R. B. Metcalf and S. D. M. White. Cosmological information in the gravitational lensing of pregalactic HI. *MNRAS*, 394:704–714, April 2009.

[4] W. Hu. Mapping the Dark Matter through the Cosmic Microwave Background Damping Tail. *ApJ*, 557:L79–L83, August 2001.

[5] P. Dewdney. SKA1 System Baseline Design. *SKA Project Documents*, pages 1–98, 2013.

[6] A. Pourtsidou and R. B. Metcalf. Weak lensing with 21 cm intensity mapping at z ∼ 2-3. *MNRAS*, 439:L36–L40, March 2014.

[7] M. McQuinn, O. Zahn, M. Zaldarriaga, L. Hernquist, and S. R. Furlanetto. Cosmological Parameter Estimation Using 21 cm Radiation from the Epoch of Reionization. *ApJ*, 653:815–834, December 2006.

[8] Y. Mao, M. Tegmark, M. McQuinn, M. Zaldarriaga, and O. Zahn. How accurately can 21cm tomography constrain cosmology? *PRD*, 78(2):023529, July 2008.